Structural, morphological, and optical properties of double-ended needle-like ultra-long ZnO micro/nanorods

# Structural, morphological, and optical properties of double-ended needle-like ultra-long ZnO micro/nanorods

**R B Kale[1] and Shih-Yuan Lu[1]**

Department of Chemical Engineering, National Tsing-Hua University, Hsinchu 30043, Taiwan, Republic of China

E-mail: rb_kale@yahoo.co.in and sylu@mx.nthu.edu.tw

**Abstract**

An environmentally benign hydrothermal route was used to synthesize ultra-long double-ended needle-like ZnO microrods. The microrods were morphologically uniform with a diameter of around 1–2 $\mu$m, and a length of 40–50 $\mu$m. The rods were grown directly from an aqueous alkaline solution containing $Zn(OH)_4^{2-}$ ions, produced from $ZnSO_4$ and NaOH, without using any structure-directing reagent. The products were characterized using x-ray diffraction, energy-dispersive x-ray analysis, scanning electron microscopy, ultraviolet–visible spectrophotometry, and photoluminescence, and the results are reported. The influence of the preparation parameters on the morphology of the ZnO products is also discussed.

(Some figures in this article are in colour only in the electronic version)

## 1. Introduction

To control the morphology and size is a matter of considerable importance in the manufacture of microcrystalline powders. In many applications, not only the size but also the shape plays an important role in determining the usefulness of the products. However, the formation mechanism of and transformation between the different morphological forms of the same substance are still a topic of extensive discussion [1]. Zinc oxide (ZnO) is a much studied material due to its non-toxicity, inexpensive production, and easy to grow nature. ZnO is a transparent wide direct band gap (3.37 eV) semiconductor with a large exciton binding energy (60 meV), much larger than that of other prospective materials such as ZnSe (22 meV), GaN (25 meV), and ZnS (40 meV), which makes it one of the most outstanding candidates for special optoelectronic devices [2]. Polycrystalline/nanocrytalline ZnO has potential applications in

---

[1] Authors to whom any correspondence should be addressed.

room-temperature ultraviolet (UV) lasers, piezoelectric transducers, field emission, light-emitting diodes, phosphors, gas sensors, solar cells, acoustic waveguides, etc [3–10].

Nowadays, chemical vapour deposition (CVD) and solution phase methods are widely used for fabricating ZnO nanostructures and/or microstructures [11–17]. Solution phase syntheses have attracted considerable attention due to their mild reaction conditions, low operating temperature, environmental benignancy, simplicity, large-scale production, easy to control preparation parameters, etc. But most of the ZnO products synthesized using solution phase methods have been flowerlike or hierarchical nano/microstructures and they still face the problem of polydispersity. The synthesis of individual microrods has rarely been reported. In fact, to the best of our knowledge, the preparation of uniform ZnO microrods with high aspect ratios has not been reported.

In the present work, we report a simple hydrothermal method to grow well-crystallized individual ZnO microrods using an aqueous alkaline solution containing zinc ions and sodium hydroxides. To study the photoluminescence properties, the products were excited with light of different wavelengths.

## 2. Experimental details

The ZnO microrods were synthesized using a precursor solution consisting of zinc sulfate ($ZnSO_4$) and NaOH (sodium hydroxide), prepared in deionized water (Milliq, 18.2 M$\Omega$). In the present synthesis process, 60 ml of $ZnSO_4$ (0.025 M) was added to 60 ml of NaOH (1 M). The resultant solution was stirred for a few seconds and then transferred to a Teflon-lined stainless steel autoclave of 500 ml capacity (only 24% of the total volume of the autoclave was filled with the solution). The autoclave was maintained at 170 °C for 24 h and then cooled naturally to room temperature. The whitish product was collected from the bottom of the container, repeatedly washed with deionized water, and then dried at 80 °C for 8 h.

X-ray diffraction (XRD) patterns were obtained using a Phillips x-ray diffractometer equipped with high-intensity Cu K$\alpha$ radiation ($\lambda = 1.5417$ Å) in the $2\theta$ range of 20°–75°. Scanning electron microscope (SEM) images were obtained using a JEOL JSM-5600, equipped with an energy-dispersive x-ray analyser (EDAX). Optical absorption spectra were recorded using an ultraviolet–visible (UV–vis) spectrophotometer (Hitachi Model-330, Japan). Room-temperature photoluminescence (PL) spectra were obtained on a Hitachi F-4500 fluorescence spectrophotometer with a xenon lamp (150 W) as the excitation source. Different excitation wavelengths were used for the PL measurements.

## 3. Results and discussion

The XRD pattern of the as-synthesized microrods is illustrated in figure 1(a). The obtained ZnO microrods are of the hexagonal (wurtzite-type) structure with lattice constants of $a = 3.254$ and $c = 5.239$ Å. All the diffraction peaks of the ZnO microrods were shifted towards lower angles, as compared with the standard values (JCPDS file no 36-1451), suggesting an increase in the interplanar distances. This may be attributed to the existence of tensile stress in the lattice of the ultra-long ZnO microrods. The sharp peaks with low FWHM reveal the well-crystallized nature of the ZnO microrods.

Figure 1(b) shows a representative EDAX pattern and the details of the relevant elemental analysis for the ZnO microrods. The pattern shows strong Zn and O peaks without any impurity peaks, confirming the high purity of the ultra-long ZnO microrods. The average atomic ratio for Zn versus O was found to be 48.3:51.7, indicating that the product was in good stoichiometric ratio within experimental error.
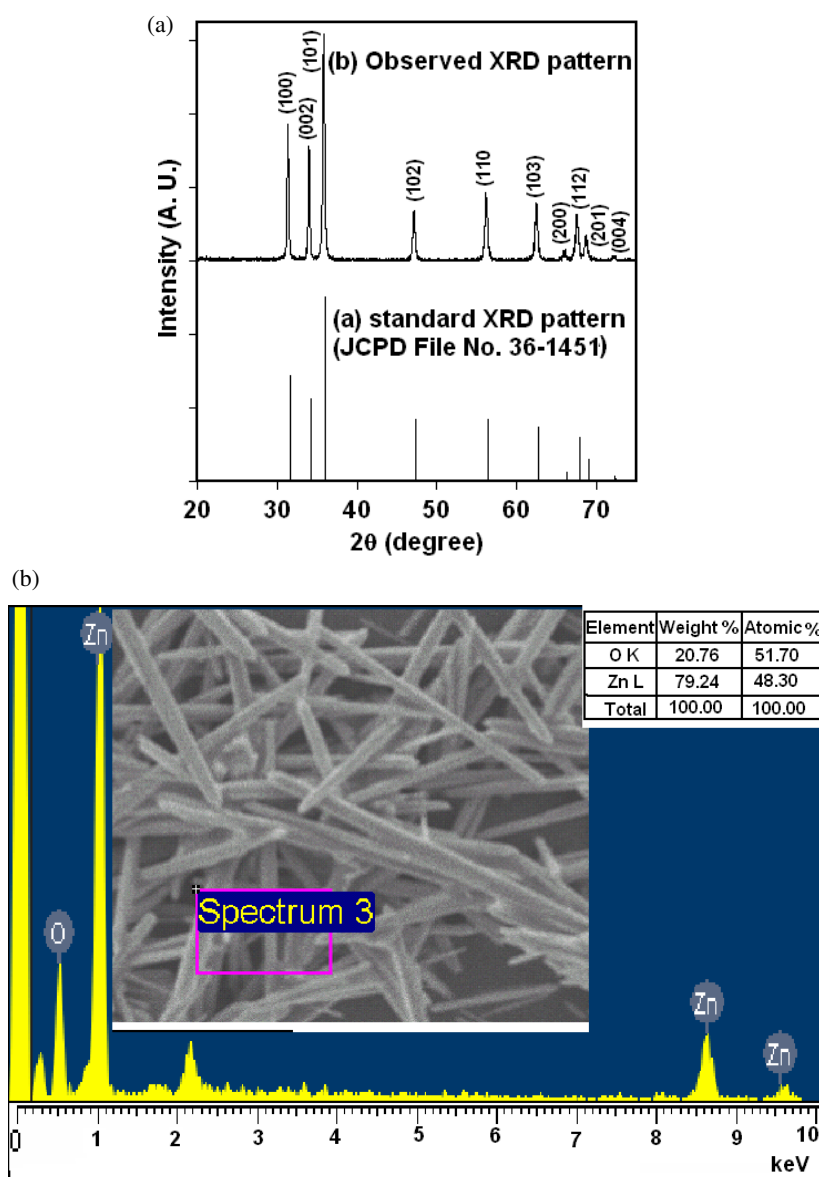
**Figure 1.** (a) XRD pattern of ZnO microrods. (b) A typical EDAX pattern of ZnO microrods. The inset shows the EDAX analysis and the region selected for elemental analysis.

Figures 2(a)–(c) shows the SEM images of the as-synthesized ZnO products with different magnifications. Low-magnification SEM images clearly show that the product was in the form of microrods of high morphological yield. The microrods were grown individually and have a diameter of 1–2 $\mu$m and a length of 40–50 $\mu$m, giving a high aspect ratio. The microrods have sharp tips to their both ends (figure 3), indicating that the growth of the microrods is different from the idealized growth habit of the ZnO crystal under hydrothermal condition [18]. The growth habit of the present ZnO product may be attributed to the lower concentration of the zinc species in the solution and less hydrothermal pressure acting on the ZnO nuclei during
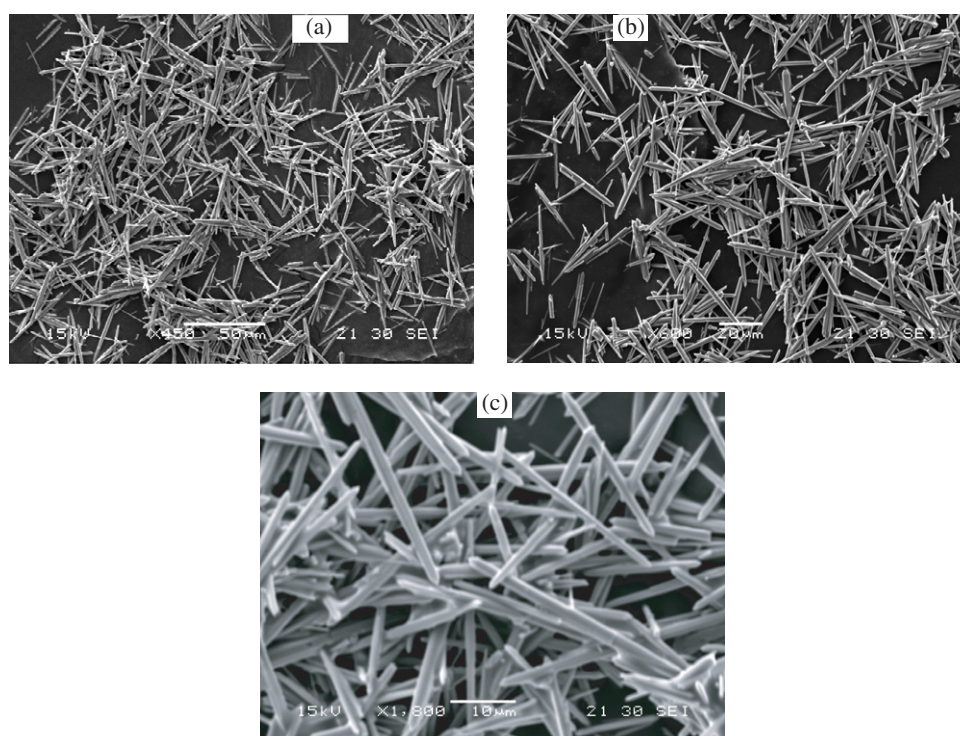
**Figure 2.** (a)–(c) SEM images of ZnO microrods with different magnifications.

the growth process, since only 24% of the total volume of the autoclave was filled with the solution.

The overall reaction procedure for growing ZnO microrods in an aqueous alkaline solution is proposed below:

$$Zn^{2+} + 2OH^- \rightarrow Zn(OH)_2 \tag{1}$$

$$Zn(OH)_2 + 2OH^- \rightarrow Zn(OH)_4^{2-} \tag{2}$$

$$Zn(OH)_4^{2-} \rightarrow ZnO + H_2O + 2OH^-. \tag{3}$$

At the early stage, initially grown ZnO nuclei, formed from the decomposition of $Zn(OH)_4^{2-}$, can act as the seed nuclei, and newly formed species adsorbed onto them can enhance the anisotropic growth that results in the formation of microrods. It is well known that, under the aqueous alkaline condition, polar growth of ZnO crystal along the $\langle 001 \rangle$ directions proceeds through the adsorption of growth units of $Zn(OH)_4^{2-}$ onto the (001) plane, resulting in an anisotropic growth. The growth of the present microrods may be attributed to the low concentration of zinc species and lower pressure during the hydrothermal growth.

Under the same experimental conditions, except that the concentration of $ZnSO_4$ was increased from 0.025 to 0.05 M, the obtained product (figure 4(a)) was in the form of nanorods with diameter of 200–250 nm and length of 6–8 $\mu$m, possessing a high aspect ratio of larger than 50 (with some diversity not shown here). This reveals that the growth habits of the ZnO crystal are different (inset of figure 4(a)), due to the increase in concentration of Zn ions and the consequent decrease in pH value. When the concentration of $ZnSO_4$ was increased to 0.05 M and that of NaOH was decreased to 0.5 M, the product became flowerlike (figure 4(b)), and these ZnO flowers were composed of many nanorods of diameter around 100–125 nm and
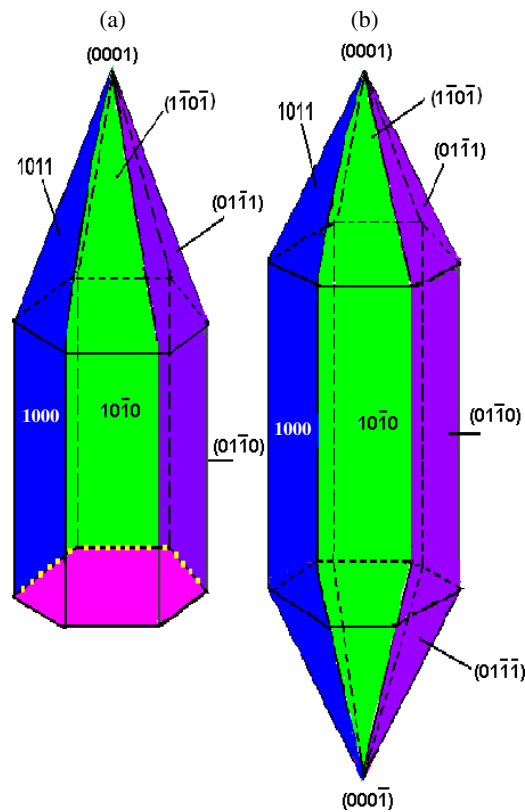
**Figure 3.** (a) Idealized hydrothermal growth of ZnO crystals. (b) Hydrothermal growth under present experimental conditions.
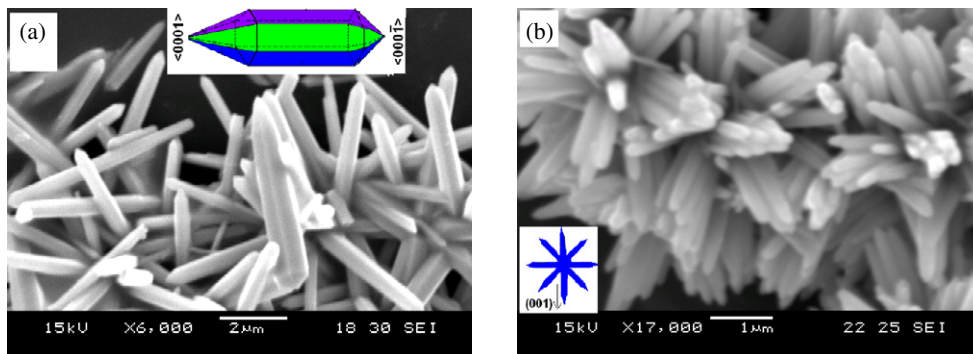


**Figure 4.** SEM images of ZnO products produced from (a) 0.05 M $ZnSO_4$, 1 M NaOH and (b) 0.05 M $ZnSO_4$, 0.5 M NaOH, for reported reaction time and temperature.

length in the range of 1.5–2 $\mu$m (aspect ratio >15), indicating that the preparation parameters were the key factors for growing ZnO crystals with different morphology.

Room-temperature absorption and PL studies of the ZnO product were performed by ultrasonically dispersing the samples in spectroscopic-grade ethanol. Photoluminescence spectra of microrods were measured at different excitation wavelengths (275, 300 and 325 nm)
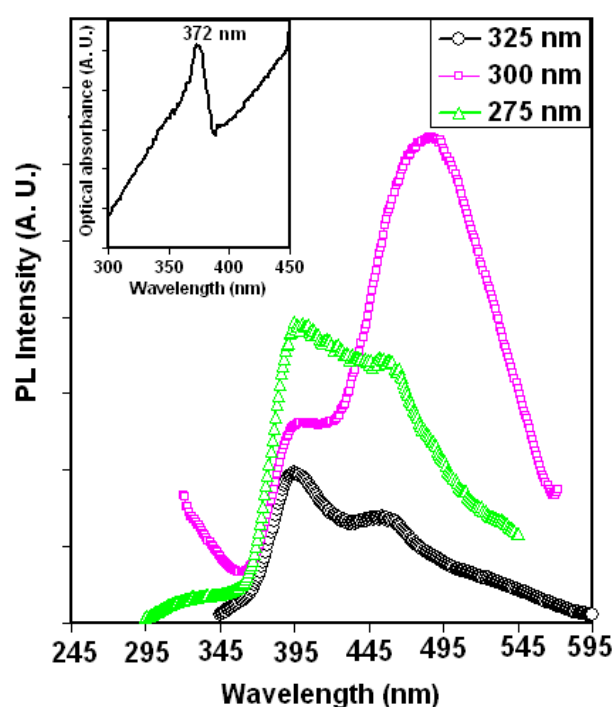
**Figure 5.** PL spectra of ZnO microrods at different excitation wavelengths. The inset shows the optical absorption spectrum.

and the results are shown in figure 5. If the microrods were excited with wavelengths 275 and 325 nm, one found an ultraviolet (UV) emission peak centred at 396 nm and a blue emission peak at 462 nm. Ge *et al* observed [19] an ultraviolet emission peak centred at 404 nm for the three-dimensional (3D) ZnO nanostructures they prepared and explained that the emission may be attributed to the radiative recombination between the electrons in the conduction band and the holes in the valence band. They also mentioned that the spectrum showed a redshift of about 20 nm as compared with the previously reported near band edge emissions of ZnO products, and argued that the PL spectrum of ZnO is sensitive to the particle shape, size, temperature, and method of preparation, etc. Fu *et al* [20] also observed UV emissions centred at 392 nm after annealing ZnO films deposited on Si substrates. When the present product was excited with 300 nm light, the blue emission disappeared while a strong blue-green emission peak of 492 nm appeared, with the UV emission peak still present. This type of result had been reported by Zhang *et al* for rf-sputtered ZnO thin films [21]. Previously, it was reported [22–26] that the blue and blue-green emission peaks are due to singly ionized oxygen vacancies or surface defects. However, the mechanism is not yet clear for these emissions [27–29]. The UV–vis absorption spectrum of the ZnO microrods (inset of figure 5) clearly indicates the excitonic characteristic of the ZnO microrods at room temperature. The absorption peak was centred at 372 nm, which is in good agreement with the previously reported value [30].

## 4. Conclusion

Ultra-long ZnO microrods were synthesized using a simple hydrothermal route. The as-synthesized ZnO microrods had well-crystallized hexagonal structure. The PL emissions

exhibited ultraviolet, blue, and blue-green emission peaks depending on the excitation wavelength. When the excitation wavelength was 275 or 325 nm, one observed an ultraviolet emission at 396 nm and a blue emission at 462 nm, but at the excitation wavelength of 300 nm one observed a very strong blue-green emission at 492 nm in addition to the ultraviolet emission.

## Acknowledgments

## References

[1] McBride R A, Kelly J M and McCormack D E 2003 *J. Mater. Chem.* **13** 1196
[2] Shen G, Bando Y, Chen D, Liu B, Zhi C and Golberg D 2006 *J. Phys. Chem.* B **110** 3973
[3] Tang Z K, Wong G K L, Yu P, Kawasaki M, Ohtomo A, Koinuma H and Segawa Y 1998 *Appl. Phys. Lett.* **72** 3270
[4] Kadota M and Miura T 2002 *Japan. J. Appl. Phys.* **41** 3281
[5] Liu C, Zapien J A, Yao Y, Meng X, Lee C S, Fan S, Lifshitz Y and Lee S T 2003 *Adv. Mater.* **15** 838
[6] Service R F 1997 *Science* **276** 895
[7] Hosono E, Fujihara S and Kimura T 2004 *Electrochem. Solid State Lett.* **7** C49
[8] Minne S C, Manalis S R and Quate C F 1995 *Appl. Phys. Lett.* **67** 3918
[9] Keis K, Vayssieres L, Lindquist S E and Hagfeldt A 1999 *Nanostruct. Mater.* **12** 2595
[10] Gorla C R, Emanetoglu N W, Liang S, Mayo W E, Lu Y, Wraback M and Shen H 1999 *J. Appl. Phys.* **85** 2595
[11] Wang Y H, Wang B, Xu N S and Wang G W 2006 *Appl. Phys. Lett.* **89** 013108
[12] Zhao D, Liu Y, Shen D, Lu Y, Zhang L and Fan X 2003 *Appl. Phys. Lett.* **94** 5605
[13] Jain J K, Wang C, Zhang Z H, Chen X L, Xu L U and Wang T M 2006 *Mater. Lett.* **60** 3809
[14] Kim S W, Fujita S, Park H K, Yang B, Kim H K and Yoon D H 2006 *J. Cryst. Growth* **292** 306
[15] Zhang J, Sun L, Yin J, Su H, Liao C and Yan C 2002 *Chem. Mater.* **14** 4172
[16] Sun Y, Angwafor N, Riley D J and Ashfold M N R 2006 *Chem. Phys. Lett.* **431** 352
[17] Meng X, Lin B, Gu B, Zhu J and Fu Z 2005 *Solid State Commun.* **135** 411
[18] Li W J, Shi E W, Zhong W Z and Yin Z W 1999 *J. Cryst. Growth* **203** 186
[19] Ge J, Tang B, Zhuo L and Shi Z 2006 *Nanotechnology* **17** 1316
[20] Fu Z X, Guo C X, Lin B X and Liao G H 1998 *Chin. Phys. Lett.* **15** 457
[21] Zhang D H, Wang Q P and Xue Z Y 2003 *Appl. Surf. Sci.* **207** 20
[22] Vanheusden K, Warren W L, Seager C H, Tallant D R, Voigt J A and Gnade B E 1996 *J. Appl. Phys.* **79** 7983
[23] Xue Z Y, Zhang D H, Wang Q P and Wang J H 2002 *Appl. Surf. Sci.* **195** 126
[24] Bachari E M, Baud G, Ben Amor S and Jacquet M 1999 *Thin Solid Films* **348** 165
[25] Huang M H, Wu Y, Feick H, Tran N, Weber E and Yang P D 2001 *Adv. Mater.* **13** 113
[26] Wang J Z, Du G T, Zhang Y T, Zhao B J, Yang X T and Liu D L 2004 *J. Cryst. Growth* **263** 269
[27] Wu J J and Liu S C 2002 *Adv. Mater.* **14** 215
[28] Fu Z, Lin B, Liao G and Wu Z 1998 *J. Cryst. Growth* **193** 316
[29] Wang J and Gao L 2004 *J. Cryst. Growth* **262** 290
[30] Liu B 2004 *Langmuir* **20** 4196